Available online at www.jourcc.com

Journal homepage: www.JOURCC.com

Journal of Composites and Compounds

Chemical, thermal, and microstructural characterization of polyethylene terephthalate composites reinforced with steel slag geopolymer waste

Eliziane Medeiros Santos [a], Flávio James Humberto Tommasini Vieira Ramos [b], Pedro Henrique Poubel Mendonça da Silveira [a], Sérgio Neves Monteiro [a], Alaelson Vieira Gomes [a]*

[a] *Department of Materials Science, Military Institute of Engineering (MIE), 22290-270, Rio de Janeiro, Brazil*
[b] *Instituto de Macromoléculas Professora Eloisa Mano, Universidade Federal do Rio de Janeiro, 21941-598, Rio de Janeiro, Brazil*

ABSTRACT

The search for sustainable materials has grown globally due to the struggle against environmental impacts. From the recycling of PET packaging and the use of steel mill slag residue, from the steel production, it was developed in this work composites of PET matrix with additions of geopolymer obtained from steel mill slag. The composites were produced with concentrations of 0, 20, 40, and 60% of geopolymer and were characterized by XRD, FTIR, TGA, DSC, and SEM. The XRD analyses indicated the presence of mineral constituents referring to the geopolymer in the composites. Through the thermal analyses, it was observed that the addition of geopolymer promoted the increase in thermal stability, besides increasing the crystallinity in concentrations of 40 and 60% of geopolymer. From the micrographs, it was observed that the addition of reinforcement changed the morphology of the material, promoting an increase in the porosity of the material. From the characterizations, it is possible to state that the addition of geopolymers in the PET matrix produces low-cost composites with good properties and can be used in engineering applications. ©2021 JCC Research Group.
Peer review under responsibility of JCC Research Group

ARTICLE INFORMATION

Article history:
Received 17 June 2021
Received in revised form 23 July 2021
Accepted 29 August 2021

Keywords:
PET Composites
Geopolymer
Steel Slag Waste
Thermal Characterization
Waste Reuse
Chemical Characterization

1. Introduction

With the advances in urbanization and industrialization, solid waste is generated. Annually, about 1.3 billion tons of solid waste are generated worldwide. This waste, if not treated correctly, becomes one of the most harmful pollutants, and its incorrect disposal generates great environmental impacts. Among these wastes is plastic waste that is not biodegradable and remains in nature for centuries, causing a major environmental problem. Polyethylene terephthalate, better known as PET, accounts for 18% of the world's plastic production. Steel mill waste also enters this solid waste and contributes to this problem. It is estimated that about 400 tons of steel mill waste is generated annually and for every ton of steel produced 450 kg of co-products and waste such as scoria are generated [1–5].

PET is a thermoplastic polymer that has a melting temperature of 265 °C, is easily found, has plasticity (which provides better workability) and its reuse helps reduce environmental impacts. One of the problems that can arise in the processing of a thermoplastic is its multiple processing that can lead to degradation of the material [6].

Several types of research seek to develop processes that introduce PET into other materials, to obtain new products with long useful life and high added value since plastics are villains when the subject is global urban solid waste. One of the most important benefits of using recycled PET is to have cleaner management of waste materials [7,8].

Steel slag is one of the most common types of industrial waste. It is a by-product of steel making. SS is produced during the separation of the molten steel from impurities in steelmaking furnace. The production of one tonne of steel tends to produce about 130–200 kg of SS, depending on steel production process and the composition of steel [9-11]. The large unused portion was deposited in areas adjacent to the steel manufacturing plants, occupied a large amount of farms and polluted environment [12]. Steel slag has been widely used in different materials with good results. The basic composition of steel slag is metallic and non-metallic oxides and the types are differentiated by the generation process. They can be used in the manufacture of different types of materials and with geopolymerization studies have already been done to create binders, mortars, and different types of concrete. Although there are already studies on the reuse of steel slag, there is still a large amount

* *Corresponding author: Eliziane Medeiros Santos; E-mail:elizianemsantos@gmail.com*
DOR: 20.1001.1.26765837.2021.3.8.3.0
https://doi.org/10.52547/jcc.3.3.3

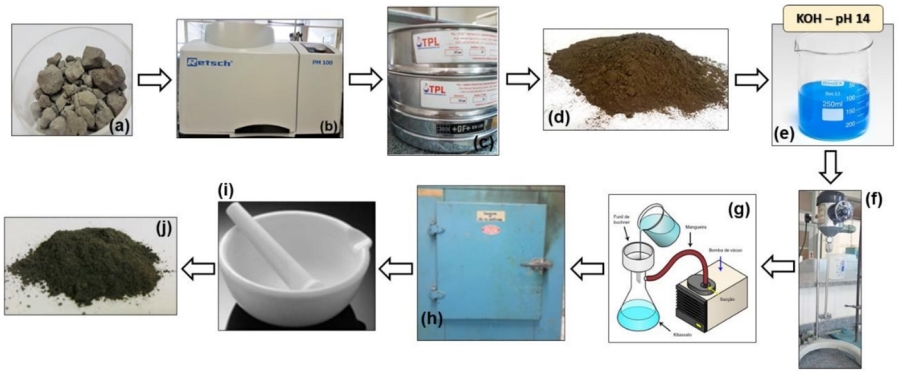

Fig. 1. Geopolymer preparation process: (a) steel slag as received; (b) agitation in a high energy mill for 90 min; (c) 63µm sieve step; (d) sieved steel slag; (e) KOH solution; (f) agitation of steel slag in KOH solution for 24h; (g) vacuum filtration to remove impurities; (h) oven drying 80 °C/24h; (i) deagglomeration of geopolymer powders; (j) obtaining geopolymer powder.

Table 1.
Composition of the steel slag

FeT (%)	Fe0 (%)	FeO (%)	CaO (%)	SiO_2 (%)	MgO (%)	MnO (%)	Al_2O_3 (%)	S (%)	ZnO (%)	K_2O (%)	Na_2O (%)
53.58	32.03	26.42	17.30	7.11	5.35	2.09	3.97	0.68	<0.005	0.26	0.08

of slag stored, hence the need to find other applications to facilitate environmental protection [13-15]. Steel slag is a residue that has potential application in several applications, being highly used as an alternative to traditional materials. As an example, steel slag is used as an additive to improve the physicochemical properties of the soil, increasing its pH [16]. It can also be used to decrease demand for liming in acidic soil [17,18], production of ecological potassium silicate fertilizer [19], can be used in road construction because of its high hardness and good cementitious properties [20,21]. Steel slag can also replace clinker in cement plants and as part of the aggregate [22], it can be used to treat industrial wastewater to remove phosphorus, aqueous ammonium, nitrogen, phenol and arsenic [23,24]. However, its application as a precursor in the synthesis of geopolymers followed by acting as a reinforcement phase in polymeric matrix composites is something rarely found in the literature in general.

Geopolymers are semi-crystalline materials derived from the reaction of an aluminosilicate precursor with a concentrated solution of sodium silicate or alkali metal hydroxide [25,26]. The value of geopolymer technology lies in its ability to produce high-performance binders from waste materials such as fly ash, blast furnace slag, steel mill slag, metakaolin, rice husk ash, red mud, among others [27]. The transformation of these industrial wastes into products for structural and/or engineering applications has been explored. Geopolymers produced from slag have been reported as one of the most promising sustainable building materials of the 21st century [28,29].

The concept of geopolymer synthesis is based on the composition of an aluminosilicate network composed of tetrahedral $[AlO_4]^{5-}$ and octahedral $[SiO_4]^{4-}$ units that are derived from the reaction between an alkaline activator and the precursor aluminosilicate precursors. These materials can be of natural origin, such as natural clays, or of artificial origin, such as industrial waste and its by-products [30,31]. The synthesis of geopolymers occurs by alkaline dissolution followed by precipitation in aqueous solution. After a certain period, the material undergoes stiffening and the strength of the geopolymer is achieved. Thus, the geopolymerization reaction system has been the subject of studies by many re-searchers [1,32].

Geopolymerization is an alternative for waste reuse, where a chemical reaction of precursor materials (aluminosilicates) occurs in an alkaline medium providing a hardened material at room temperature [33]. Geopolymers were presented as a promising alternative with less environmental impact. To produce a geopolymer, the material needs to have an amorphous, metastable, or semi-crystalline fraction structure that can be dis-solved in alkaline or acidic solution to form oligomers constituting the polysialate system of the gel. In production, a mixture of waste or natural sources of aluminosilicates (such as fly ash, volcanic ash, and metakaolin) with alkaline activators (such as sodium hydroxide and sodium silicate) is made. With the mixture, the aluminosilicate precursors are dis-solved by the alkaline activator, releasing aluminate and silicate monomers that subsequently undergo a polycondensation reaction. The result then produces bonding gels with potentially low CO_2 footprint and high initial and thermal strength [34,35].

Geopolymers are materials that have high fire and heat resistance. It is an economical material that is corrosion resistant and has heavy metal solidification. However, it has low tensile strength and toughness. Its properties and uses have been widely explored seeking to investigate its performance [36].

The elaboration of a composite seeks to combine properties that improve the mechanical characteristics, where the pure material is not able to have. They have two phases, a matrix and a dispersed one [37]. Composite materials that have a thermoplastic matrix have greater resistance to fracture, to impact, greater tenacity, shorter processing time, are tolerant to damage and have great environmental stability [38].

Knowing that PET has plasticity, which contributes to better workability and versatility than steel slag from geopolymerization, a composite was prepared using the combination of PET and geopolymer particles, seeking to develop a sustainable material with innovative and efficient applications. The objective of this work is to process and characterize PET matrix composites, reinforced with steel slag waste geopolymers, analyzing and comparing their behavior from the variation of their composition, to qualify them in the search for future sustainable applications. From the results generated, it is expected that this composite will contribute to the reduction of solid waste generation, used in the future in the creation of new engineering materials.

2. Experimental procedure

2.1. Raw materials

The recycled PET used was provided by the company Codesfi-Rio (Rio de Janeiro, Brazil), the geopolymer obtained from geopolymerization made with steel slag, was provided by USIMINAS (Belo Horizonte, Brazil). The chemical composition of the steel slag used is described in Table 1.

2.2. Geopolymer synthesis

The PET was received in the form of post-consumption, being necessary to cut it in a knife mill, turning the material into powder. The

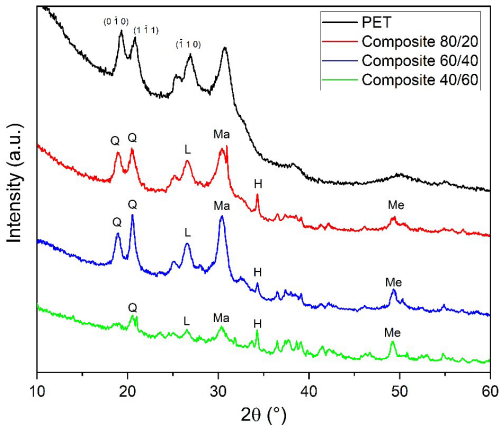

Fig. 2. X-ray diffractogram of PET and PET composites. The indicated phases on diffractogram are: Q - Quartz; Ma - Mayenite; Me - Merwinite; H - Hematite; L - Larnite.

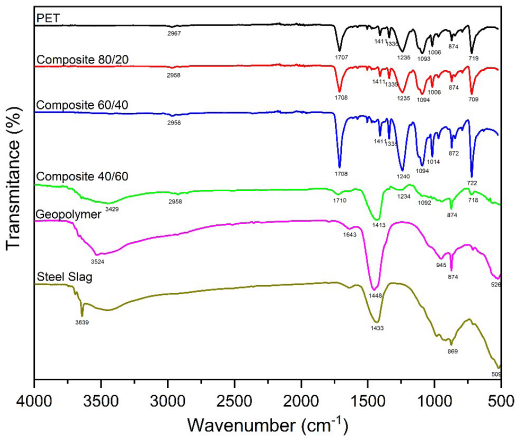

Fig. 3. Overlay of the FT-IR spectra of samples.

geopolymer was obtained from the geopolymerization of steel slag. The procedure, which is shown in Fig. 1 begins with the grinding of steel slag in a high-energy mill at 300 rpm for 90 min. After grinding, the comminuted material is sieved to a particle size of 63 μm.

The geopolymerization was performed by inserting the steel slag powders in a solution of deionized water with KOH to obtain pH 14. The powders with the alkaline solution are stirred for 24h. After the alkaline treatment, the powders went through vacuum filtration to remove impurities, followed by drying at 80 °C for 24h. After drying, the geopolymers were deagglomerated to obtain their final powder form.

2.3. Composites processing

The specimens were prepared in the compositions described in Table 2. The compo-site samples were mixed in the high energy mill at a speed of 300 rpm for 30 min. After mixing, the samples were processed by hot pressing at a temperature of 270 °C for 10 min, followed by degassing for 30 sec.

2.4. Characterization

2.4.1. X-ray diffraction (XRD)

The crystalline phases of the composites with geopolymer and the planes found in pure PET were identified by X-ray diffraction analysis. The analysis was performed in a PANalytical diffractometer, model XPert Pro MRD (Malvern Panalytical, São Paulo, Brazil), operated with a CoKα source (λ=1.789 Å), 40 mA current, 45 kV voltage, 2θ range from 10° to 90°, 0.050° step scan and 180s of time per step.

2.4.2. Fourier transform infrared spectroscopy (FTIR)

FTIR analysis was done to study changes in the chemical bonding of geopolymers and the PET composites reinforced with geopolymers. FTIR spectra were recorded on Ni-coletiS10 equipment (Thermo Fisher Scientific, Massachusetts, USA) in the range of 400–4000 cm^{-1} with a resolution of 4 cm^{-1}. The samples were pressed, forming KBr pellets under pressure of 10 kgf/cm for 5 min.

Table 2.
List of composites sample groups

Group	PET (%)	GEOPOLYMER (%)
PET	100	0
Composite 80/20	80	20
Composite 60/40	60	40
Composite 40/60	40	60

2.4.3. Differential scanning calorimetry (DSC)

The test was carried out on Q1000 equipment from TA Instrument (New Castle, USA), in a nitrogen atmosphere with a heating rate of 10 °C/min, with a temperature range of 25 to 300 °C for PET and composites samples. From this technique, it was possible to determine the glass transition temperatures (T_g), initial temperature (T_{onset}), melting temperature (Tm), final temperature (T_{endset}), crystallization temperature during the second heating (T_{ch}), melting enthalpy (ΔH_m), and crystallinity index (X_c).

2.4.4. Thermogravimetric analysis (TG/DTG)

The thermal degradation of the composites was performed in Shimadzu DTG-60H equipment (Tokyo, Japan). The samples were crushed and placed in a platinum crucible. The procedure was performed under a nitrogen atmosphere, with a heating rate of 10 °C/min, operating at a temperature of 20 to 700 °C, according to ASTM E1131 [39].

2.4.5. Scanning electron microscopy (SEM)

The fractured surfaces of the PET/Geopolymer composite specimens and the slag and geopolymer powders were analyzed using a Quanta FEG 250, Fei microscope (Hills-boro, USA). The equipment was used with a secondary electron detector at an acceleration voltage of 5 kV. The composite samples were prepared using the cryofracture technique, where these samples are frozen with nitrogen and then fractured with the aid of a cutting tool. After the fracture, the samples were covered with gold in the Leica Ace600 equipment (Wetzelar, Germany).

3. Results and Discussion

3.1. XRD results

Fig. 2 shows the diffractograms of pure PET and the 80/20, 60/40 and 40/60 composites. In the PET diffractogram, the planes (0 0), (1 1) and (1 0) were observed in peaks 19.32, 20.84, and 26.91 2Θ, as found by Pereira et al. [40].

The diffractograms of the 80/20, 60/40, and 40/60 composites showed peaks characteristic of geopolymeric materials. Peaks referring to calcium silicate in allotropic forms such as Merwinite at peak 49.30° and Larnite at peak 26.50° were identified. The presence of the minerals Mayenite (30.35°), Hematite (34.31°), and Quartz (18.80 and 20.44°) was also observed [41-43].

3.2. FTIR results

Fig. 3 shows the absorption spectra of the samples of steel slag, geo-

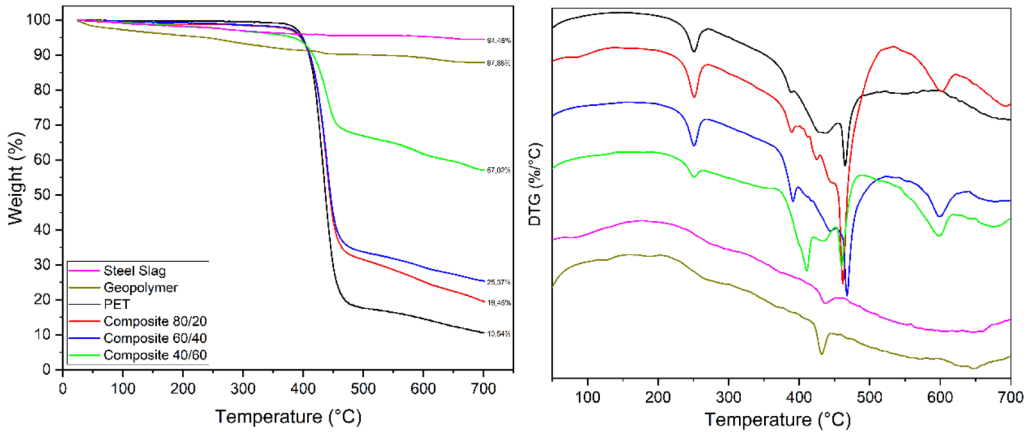

Fig. 4. TG and DTG curves for the PET and PET/Geopolymer composites.

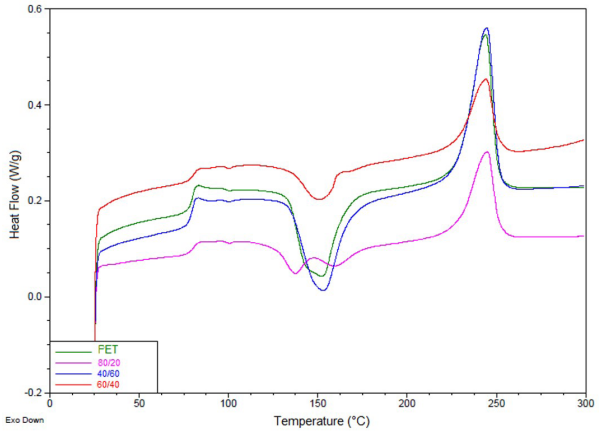

Fig. 5. DSC curves for pet and geopolymeric composites.

polymer, pure PET, and PET/Geopolymer composites. The details of the spectrum are given in the Table 3. Peaks were found referring to the OH group (3639 and 3524 cm^{-1}), symmetric stretching of the C-H bond (2958 and 2957 cm^{-1}), stretching of the C=O bond (1707, 1708, 1710 cm^{-1}), aromatic skeleton vibration with C=C bond stretching (1448, 1433, 1413 and 1411 cm^{-1}), C-O group stretching and OH group deformation (1335 cm^{-1}), terephthalate group $OOCC_6H_4$-COO (1094, 1093 and 1092 cm^{-1}), C-O stretching (1006 and 1014 cm^{-1}), Si-O bond band stretching (945 cm^{-1}), aromatic ring 1,2,4,5; substituted tetra (874, 872 and 869 cm^{-1}), the interaction of polar ester groups and benzenic rings (709, 718 and 719 cm^{-1}), Si-O bond band bending vibration (526 and 509 cm^{-1}) [40,44,45].

Table 3.
Bands with vibrational modes assigned to the FTIR spectrum of geopolymers, steel slag, and PET / Geopolymer composites

Absorption Bands (cm^{-1})	Bands
3639 and 3524	O-H, stretch
2967 and 2958	Symmetrical stretching of C-H
1707	Stretching of C=O of carboxylic acid group
1643	Stretching vibration of O-H
1411 and 1335	Stretching of the C-O group deformation of the O-H group and bending and wagging vibrational modes of the ethylene glycol segment
1235	Terephthalate Group (OOCC6 H4 -COO)
1094, 1093 and 1092	Methylene group
1014 and 1006	Methylene group and vibrations of the ester C-O bond
945	Si-O, stretch
874	Aromatic rings 1,2,4,5; Tetra replaced
719	Interaction of polar ester groups and benzene rings
526 and 509	Si–O–Si out of plane bending mode

The composites 80/20 and 60/40 showed vibrational bands similar to PET, due to this material being present in greater quantity as matrix phase. The 40/60 composite presented an absorption spectrum similar to the spectrum of pure geopolymer, with the peak at 3524 cm^{-1}, 1643 cm^{-1}, 1448 cm^{-1}, 874 cm^{-1}, and 526 cm^{-1}. This change in the characteristic feature of the 40/60 composite band occurs due to the high addition of geopolymer in the composition, where the composite begins to lose its characteristics from the polymer matrix, beginning to exhibit cementitious properties.

3.3. TG/DTG results

Fig. 4 shows the TG and DTG plots of geopolymer, steel slag, PET, and composites. When the temperature of PET is raised, its mass is reduced significantly, as expected of thermoplastic polymers at the 700 °C plateau. From the DTG plot and the results in Table 4, it is observed that the T_{max} of PET is 436.28 °C. As the PET used in this work comes from recycling, the residue generated in the characterization may indicate some material that may have been incorporated during its processing.

From the TG and DTG curves of steel slag and geopolymer, it is observed the release of water that occurs at approximately 100 °C, initiating the loss of mass of these materials. The geopolymer has a higher moisture loss than the steel slag in this temperature range, resulting in greater loss of mass (5.15 % of steel slag and 12.12 % of geopolymer). At 429.17 °C, CaOH decomposition occurs, followed by a peak corresponding to dehydroxylation of SiO_2 at 577.01 °C [48]. The mass loss of the PET/Geopolymer composites comes from the degradation of PET. The result corresponding to the higher mass loss for the pure polymer was already predicted. With the addition of geopolymer in the matrix, the shift of the degradation temperature to higher levels was observed for the 80/20, 60/40 and 40/60 composites. The T_{onset} of PET was observed at 380.71 °C. As expected, as from the incorporation of geopolymeric filler content, there was a displacement of the composite's curves to higher temperatures equivalent to 383.47 °C (80/20), 381.3 °C (60/40) and 387.05 °C (40/60). The absence of mass loss in the ladle steel slag and geopolymer was already expected since these materials do

Table 4.
TG/DTG properties of the specimens

Samples	T_{onset} (°C)	T_{max} (°C)	T_{end} (°C)	Residues (%)
PET	380.71	436.28	473.76	10.54
Steel Slag	25.00	-	700.00	94.45
Geopolymer	25.00	-	700.00	87.88
Composite 80/20	383.47	440.48	468.77	19.45
Composite 60/40	381.30	439.56	468.96	25.37
Composite 40/60	387.05	440.77	465.87	57.02

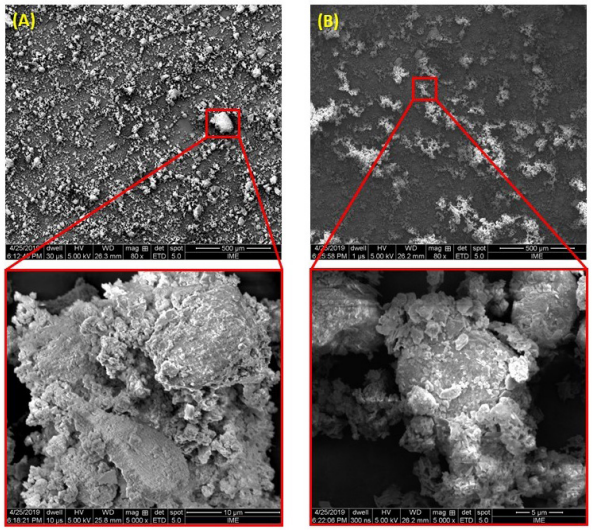

Fig. 6. SEM micrographs of powders: (a) Steel Slag; (b) Geopolymer.

not have significant degradation in the range of 25 to 700 °C.

3.4. DSC results

Fig. 5 and Table 5 indicates the results obtained from the differential scanning calorimetry (DSC) test of the materials used in this study. The DSC curves of the geopolymer composites indicate T_m like that of pure PET, but the 80/20 composite showed a reduction in the intensity of the heat flux, when compared to the other samples. The 40/60 composite presented two peaks at the temperatures of 164.63 and 197.37 °C, referring to water loss from the geopolymer and its dihydroxylation [49].

The T_{onset} of the 80/20 and 60/40 composites showed a reduction of 10.9 °C and 8.4 °C respectively. This reduction in T_{onset} is due to the early onset of degradation of the geopolymer, as can also be seen in Fig. 4. The 60/40 composite, on the other hand, presented a reduction of 2.8 °C in T_{onset}, in the same range as PET pure.

In the second DSC heating curve, an unexpected behaviour of the materials was observed. It was possible to obtain the Tg of PET and composites, being according to Romão et al. [6], that the Tg of PET corresponds to 70 °C. The DSC results showed Tg value for PET of 74.5 °C, followed by 73.1 for the 80/20 composite, 72.8 °C for 60/40 and 76.2 °C for 40/60. During heating, the 80/20 composite showed two different peaks indicating Tch (137.2 and 159.9 °C). The Tm of the PET samples and composites remained in the same temperature range.

The results concerning the degree of crystallinity indicate that the addition of geo-polymer in the matrix increased the crystallinity at additions of 40 and 60%. In the 80/20 composite, there was a reduction in the crystallinity of the material.

Table 5.
DSC results of the specimens

Samples	T_g (°C)	T_{ch} (°C)	T_{onset} (°C)	Tm (°C)	T_{endset} (°C)	ΔH_m	X_c (%)
PET	74.5	151.7	227.0	246.6	261.1	32.4	23.1
Composite 80/20	73.1	137.2 / 159.9	216.1	247.0	262.0	21.81	19.5
Composite 60/40	72.8	152.80	218.6	246.9	261.2	39.35	46.8
Composite 40/60	76.2	150.5	224.2	245.85	258.5	16.84	30.1

3.5. Microstructures

Fig. 6 shows SEM micrographs of the steel slag and geopolymer at 80 and 5000x. The steel slag powders have a smaller particle size than the geopolymers because of the sieving process during synthesis. Fig. 7 shows the fracture surfaces of the geopolymer composites after processing.

From the images, it is observed that the addition of geopolymer reinforcement in the matrix promoted the formation of pores during hot pressing, hindering the processing of composites with higher additions of geopolymer, as reported by Santos et al. [37]. The 80/20 and 60/40 composites exhibit geopolymer particles encapsulated within the polymeric matrix, unlike the 40/60 composite, where the matrix performs the function of binder of the reinforcements.

The porosity created in the composites is the result of the release of gases during the melting of PET processing for molding the specimens, however, there may be some influence of the release of free water present in the filling, as observed by the results of thermo-gravimetry. The greater porosity observed in the image of the 40/60 composite may suggest that the covered filling interfered with the gas released by the melting of the PET [46].

4. Conclusions

The geopolymer composites showed by the XRD results phases related to the minerals constituting the geopolymers, except for the 40/60 composite that did not show hematite. The incorporation of geopolymer in the matrix promoted the integration of functional groups of the steel slag and geopolymer to the PET matrix. The TGA analyses indicated an increase in the thermal stability of the composites due to the high thermal stability of the geopolymer, resulting in considerable reductions in mass loss. The 60/40 and 40/60 composites exhibited increased crystallinity

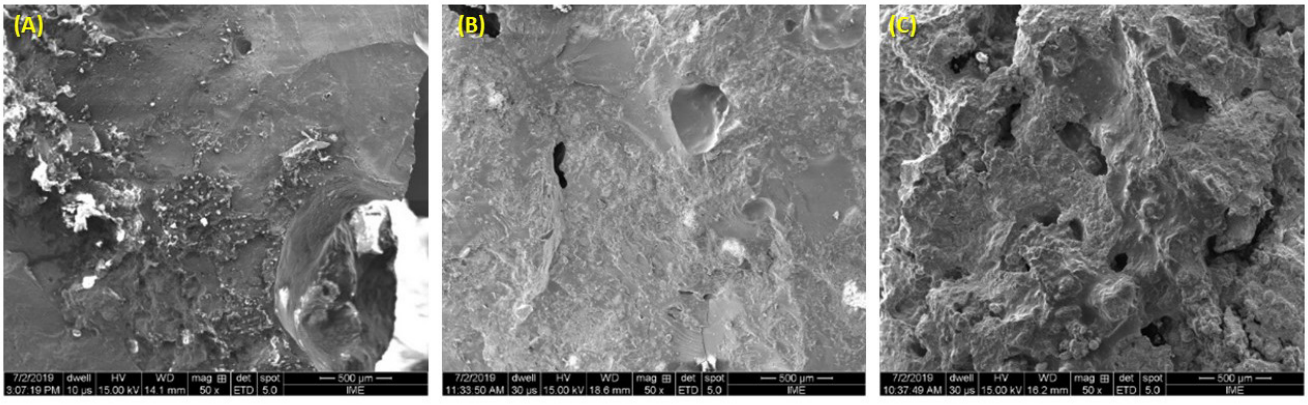

Fig. 7. SEM micrographs of fracture surface of the PET/Geopolymer composites: (a) 80/20; (b) 60/40; (c) 40/60.

by the addition of geopolymer filler, while the 80/20 composite showed a reduction in crystallinity, with a lower value than pure PET. The addition of reinforcing filler to the composite resulted in an apparent increase in the porosity of the material, seen through the SEM images. The 40/60 composite presented morphology like a ceramic, where PET acts in this composite as a binder, while in the 80/20 and 60/40 composites, the reinforcements are arranged as particles within the thermoplastic matrix. For application in future work, a study using geopolymer variations in PET different from those used in this article (10%, 15%, 30%, 50%, 70 %, …) will provide a detailed view of the thermal, chemical and microstructural properties of Geopolymer-reinforced PET matrix composites.

Acknowledgements

The authors thank the Macromolecules Institute (IMA/UFRJ) for their cooperation in thermal analysis. The authors are grateful to Codesfi-Rio and USIMINAS for donating PET slag and steelmaking waste used in this work. This study was financed in part by the Coordenação de Aperfeiçoamento de Pessoal de Nível Superior-Brasil (CAPES) - Finance Code 001.

Conflict of Interest

The authors declare that they have no conflict of interest.

REFERENCES

[1] S. Wang, W. Yan, F. Zhao, Recovery of Solid Waste as Functional Heterogeneous Catalysts for Organic Pollutant Removal and Biodiesel Production, Chemical Engineering Journal 401 (2020) 126104.
[2] A.W. Bhuiya, M. Hu, K. Sankar, P.F. Keane, D. Ribero, W.M. Kriven, Bone Ash Reinforced Geopolymer Composites, Journal of American Ceramic Society 104(6) (2021) 2767-2779.
[3] F.U.A. Shaikh, Tensile and Flexural Behaviour of Recycled Polyethylene Terephthalate (PET) Fibre Reinforced Geopolymer Composites, Construction and Building Materials 245 (2020) 118438.
[4] G. Tang, X. Liu, L. Zhou, P. Zhang, D. Deng, H. Jiang, Steel Slag Waste Combined with Melamine Pyrophosphate as a Flame Retardant for Rigid Polyurethane Foams, Advanced Powder Technology 31(1) (2020) 279-286.
[5] N. Cristelo, J. Celho, T. Miranda, Á. Palomo, A. Fernández-Jiménez, Alkali Activated Composites – An Innovative Concept Using Iron and Steel Slag as Both Precursor and Aggregate, Cement and Concrete Composites 103 (2019) 11-21.
[6] W. Romão, M.A.S. Spinacé, M.A. Paoli, Poli(Tereftalato de Etileno), PET: Uma Revisão Sobre Os Processos de Síntese, Mecanismos de Degradação e Sua Reciclagem, Polímeros 19(2) (2009) 121-132.
[7] R. Noroozi, G. Shafabakhsh, A. Kheyroddin, A. Mohammadzadeh Moghaddam, Investigating the Effects of Recycled PET Particles, Shredded Recycled Steel Fibers and Metakaolin Powder on the Properties of RCCP, Construction and Building Materials 224 (2019) 173-187.
[8] M. Asensio, P. Esfandiari, K. Núñez, J.F. Silva, A. Marques, J.C. Merino, J.M. Pastor, Processing of Pre-Impregnated Thermoplastic Towpreg Reinforced by Continuous Glass Fibre and Recycled PET by Pultrusion, Composites Part B: Engineering 200 (2020) 108365.
[9] N. Faraone, G. Tonello, E. Furlani, S. Maschio, Steelmaking slag as aggregate for mortars: effects of particle dimension on compression strength, Chemosphere 77(8) (2009) 1152-1156.
[10] E. Furlani, G. Tonello, S. Maschio, Recycling of steel slag and glass cullet from energy saving lamps by fast firing production of ceramics, Waste Management 30(8-9) (2010) 1714-1719.
[11] A.M. Rashad, A synopsis manual about recycling steel slag as a cementitious material, Journal of Materials Research And Technology 8(5) (2019) 4940-4955.
[12] P. Górak, P. Postawa, L.N. Trusilewicz, Lightweight Composite Aggregates as a Dual End-of-Waste Product from PET and Anthropogenic Materials, Journal of Cleaner Production 256 (2020) 120366.
[13] D.D. Burduhos Nergis, M.M.A.B. Abdullah, P. Vizureanu, M.F.M. Tahir, Geopolymers and Their Uses: Review, IOP Conference Series: Materials Science and Engineering 374 (2018) 012019.
[14] Z. Leng, R.K. Padhan, A. Sreeram, Production of a Sustainable Paving Material through Chemical Recycling of Waste PET into Crumb Rubber Modified Asphalt, Journal of Cleaner Production 180 (2018) 682-688.
[15] A.M. Kennedy, M. Arias-Paić, Application of Powdered Steel Slag for More Sustainable Removal of Metals from Impaired Waters, Journal of Water Process Engineering 38 (2020) 101599.
[16] J. O'Connor, T.B.T. Nguyen, T. Honeyands, B. Monaghan, D. O'Dea, J. Rinklebe, A. Vinu, S.A. Hoang, G. Singh, M.B. Kirkham, Production, characterisation, utilisation, and beneficial soil application of steel slag: a review, Journal of Hazardous Materials 419 (2021) 126478.
[17] L. Yang, T. Wei, S. Li, Y. Lv, T. Miki, L. Yang, T. Nagasaka, Immobilization persistence of Cu, Cr, Pb, Zn ions by the addition of steel slag in acidic contaminated mine soil, Journal of Hazardous Materials 412 (2021) 125176.
[18] H. He, N.F.Y. Tam.; A; Yao, R. Qiu, W.C. Li, Z. Ye, Growth and Cd uptake by rice (Oryza sativa) in acidic and Cd-contaminated paddy soils amended with steel slag, Chemosphere 189 (2017) 247-254.
[19] F. Han, S. Yun, C. Zhang, H. Xu, Z. Wang, Steel slag as accelerant in anaerobic digestion for nonhazardous treatment and digestate fertilizer utilization, Bioresource Technology 282 (2019) 331-338.
[20] D. Paul, M. Suresh, M. Pal, Utilization of fly ash and glass powder as fillers in steel slag asphalt mixtures, Case Studies In Construction Materials 15 (2021) e00672.
[21] Q. Song, M.Z. Guo, L. Wang, T.C. Ling, Use of steel slag as sustainable construction materials: a review of accelerated carbonation treatment, Resources, Conservation and Recycling 173 (2021) 105740.
[22] T. Gao, T. Dai, L. Shen, L. Jiang, Benefits of using steel slag in cement clinker production for environmental conservation and economic revenue generation, Journal of Cleaner Production 282 (2021) 124538.
[23] J. Ju, Y. Feng, H. Li, S. Liu, C. Xu, Separation and recovery of V, Ti, Fe and Ca from acidic wastewater and vanadium-bearing steel slag based on a collaborative utilization process, Separation and Purification Technology 276 (2021) 119335.
[24] Y. Li, X. Qi, G. Li, H. Wang, Efficient removal of arsenic from copper smelting wastewater via a synergy of steel-making slag and KMnO4, Journal of Cleaner Production 287 (2021) 125578.
[25] J. Davidovits, Geopolymers, Journal of thermal analysis 37(8) (1991) 1633-1656.
[26] J.L. Provis, G.C. Lukey, J.S.J. van Deventer, Do Geopolymers Actually Contain Nanocrystalline Zeolites? A Reexamination of Existing Results, Chemistry of Materials 17(12) (2005) 3075-3085.
[27] A.P.S. Pereira, F.J.H.T.V. Ramos, M.H.P. Silva, Caracterização Estrutural de Geopolímeros Sustentáveis de Escória de Aciaria LD e Escória de Aciaria LF Com KOH, Matéria 25(3) (2020) 1-14.
[28] J. Davidovits, L. Huaman, R. Davidovits, Ancient Geopolymer in South-American Monument. SEM and Petrographic Evidence, Materials Letters 235 (2019) 120-124.
[29] S. Songpiriyakij, T. Kubprasit, C. Jaturapitakkul, P. Chindaprasirt, Compressive Strength and Degree of Reaction of Biomass- and Fly Ash-Based Geopolymer, Construction and Building Materials 24(3) (2010) 236-240.
[30] A. Aboulayt, M. Riahi, M. Ouazzani Touhami, H. Hannache, M. Gomina, R. Moussa, Properties of Metakaolin Based Geopolymer Incorporating Calcium Carbonate, Advanced Powder Technology 28(9) (2017) 2393-2401.
[31] L. Rohde, W. Peres Núñez, J. Augusto Pereira Ceratti, Electric Arc Furnace Steel Slag: Base Material for Low-Volume Roads, Transportation Research Record 1819(1) (2003) 201-207
[32] A.M.M. al Bakri, H. Kamarudin, M. Bnhussain, I.K. Nizar, W.I.W. Mastura, Mechanism and Chemical Reaction of Fly Ash Geopolymer Cement- A Review, Journal of Asian Scientific Research 1(5) (2011) 247–253.
[33] J. Singh, S.P. Singh, Geopolymerization of Solid Waste of Non-Ferrous Metallurgy – A Review, Journal of Environmental Management 251 (2019) 109571.
[34] E. Kamseu, V. Alzari, D. Nuvoli, D. Sanna, I. Lancellotti, A. Mariani, C. Leonelli, Dependence of the Geopolymerization Process and End-Products to the Nature of Solid Precursors: Challenge of the Sustainability, Journal of Cleaner Production 278 (2021) 123587.
[35] N. Ranjbar, M. Zhang, Fiber-Reinforced Geopolymer Composites: A Review, Cement and Concrete Composites 107 (2020) 103498.
[36] X. Guo, J. Yang, Intrinsic Properties and Micro-Crack Characteristics of Ultra-High Toughness Fly Ash/Steel Slag Based Geopolymer, Construction and Building Materials 230 (2020) 116965.
[37] E.M. Santos, A.V. Gomes, F.J.H.T.V. Ramos, S.N. Monteiro, Novel Sustainable Composites with Geopolymeric Steel Slag and Recycled from Packing PET, Materials Science Forum 1012 (2020) 26-31.
[38] A.S. Rahman, M.E. Hossain, D.W. Radford, Synergistic Effects of Processing and Nanofiber Reinforcement on the Mechanical and Ferroelectric Performance of Geopolymer Matrix Composites, Journal of Materials Research and Technology 7(1) (2018) 45-54.

[39] American Society for Testing Materials E 1131 - Standard Test Method for Compositional Analysis by Thermogravimetry; West Conshohocken, 2003.
[40] A.P.S. Pereira, M.H.P. Silva, É.P. Lima Júnior, A.S. Paula, F.J.H.T.V. Ramos, Processing and Characterization of PET Composites Reinforced With Geopolymer Concrete Waste, Materials Research 20 (2017) 411-420.
[41] M.G. Pimentel, A.L.R. Vasconcelos, M.S. Picanço, J.V.B. de Souza, A.N. Macêdo, Caracterização Da Escória de Alto Forno Proveniente de Resíduos Industriais Visando Seu Uso Na Construção Civil, Brazilian Applied Science Review 3(2) (2019) 895–907.
[42] O.A. Hodhod, S.E. Alharthy, S.M. Bakr, Physical and Mechanical Properties for Metakaolin Geopolymer Bricks, Construction and Building Materials 265 (2020) 120217.
[43] T. Bai, Z.G. Song, Y.G. Wu, X.D. Hu, H. Bai, Influence of Steel Slag on the Mechanical Properties and Curing Time of Metakaolin Geopolymer, Ceramics International 44(13) (2018) 15706-15713.
[44] S.G. Prasad, A. De, U. De, Structural and Optical Investigations of Radiation Damage in Transparent PET Polymer Films, International Journal of Spectroscopy 2011 (2011) 7-15.
[45] C. Cazan, M. Cosnita, A. Duta, Effect of PET Functionalization in Composites of Rubber–PET–HDPE Type, Arabian Journal of Chemistry 10(3) (2017) 300-312.
[46] J. Xiang, L. Liu, Y. He, N. Zhang, X. Cui, Early Mechanical Properties and Microstructural Evolution of Slag/Metakaolin-Based Geopolymers Exposed to Karst Water, Cement and Concrete Composites 99 (2019) 140-150.
[47] V. Matthaiou, P. Oulego, Z. Frontistis, S. Collado, D. Hela, I.K. Konstantinou, M. Diaz, D. Mantzavinos, Valorization of Steel Slag towards a Fenton-like Catalyst for the Degradation of Paraben by Activated Persulfate, Chemical Engineering Journal 360 (2019) 728-739.
[48] F.J.H.T.V. Ramos, L.C. Mendes, S.P. Cestari, Organically Modified Concrete Waste with Oleic Acid, Journal of Thermal Analysis and Calorimetry 119(3) (2015) 1895-1904.
[49] J.P. Mendes, F. Elyseu, L.J.J. Nieves, A. Zaccaron, A.M. Bernardin, E. Angioletto, Synthesis and Characterization of Geopolymers Using Clay Ceramic Waste as Source of Aluminosilicate, Sustainable Materials and Technology 28 (2021) e00264.